A variational–Green's function approach to theoretical treatment and applications of the capacitance of three-dimensional geometries

ANDREAS MANDELIS[1]
Bell Northern Research, Box 3511, Station C, Ottawa, Ont., Canada K1Y 4H7

Received June 2, 1981[2]

A combined variational–Green's function approach to the determination of the capacitance of various useful three-dimensional geometries is developed. This formalism leads to general, exact expressions for the capacitance, which can be used with all geometries provided the spatial distribution of the charge can be determined. In particular, the theory takes into account the finite thickness and unequal areas of the capacitor plates. Specific applications of the theory include circular capacitors with disc and ring-shaped charged plate geometries. Such geometries are commonly encountered in experimental set-ups for capacitive measurements of thin film thicknesses in the field of microelectronics. Numerical results indicate that the values of thin film thicknesses calculated via simplified one-dimensional formulae for the capacitance may be incorrect by more than 10%

Une approche à la détermination de la capacité de diverses géometries tridimensionnelles a été developpée, utilisant une fonction de Green combinée à une méthode variationnelle. Cette formulation conduit à des expressions générales et exactes pour la capacité. Ces expressions peuvent être utilisées quelle que soit la géométrie, pourvu que la distribution spatiale de la charge puisse être déterminée. En particulier, la théorie tient compte de l'épaisseur finie et des superficies inégales des armatures du condensateur. Des applications spécifiques de la théorie comprennent des condensateurs circulaires avec des armatures en forme de disques ou d'anneaux. De telles géométries sont communément utilisées à des fins expérimentales pour des mesures capacitatives d'épaisseurs de couches minces dans le domaine de la microélectronique. Les résultats numériques indiquent que l'erreur dans le calcul de l'épaisseur de la couche mince, obtenue en utilisant des formules simplifiées unidimensionnelles pour la capacité, peut être superieure à 10%.

Can. J. Phys., **60**, 179 (1982)

1. Introduction

Accurate measurements of thin film thickness are becoming more important in the field of microelectronics as device dimensions constantly decrease. For some materials, such as polycrystalline silicon, the electrostatic capacitance method may be the only technique available which will yield accurate measurements. In this method, thickness calculations are based on simple capacitance formulae. These are valid strictly for two infinitely thin parallel plates of equal area, separated by a dielectric slab. However, for very thin film measurements the effects of the finite thickness of the capacitor plates and the possibility of unequal plate areas ought to be taken into account, in order to ensure the utmost possible accuracy of measurement.

In this paper a formalism has been developed for the capacitance of a dielectric medium between parallel conducting plates of nonzero thickness and arbitrary area ratios. It is based on a combination of the variational (1) and the Green's function (2) methods. The present work provides accurate, closed-form expressions for the capacitance of three-dimensional geometries with various plate shapes and thin dielectrics. Compared to other computational methods previously applied to several geometries (3–8), the present technique has greater flexibility, more computational tractability, and is less cumbersome. It is well suited for application to experimental data derived from capacitance measurements of thin dielectric films.

The variational method provides upper and lower bounds on the value of the capacitance by means of trial functions for the potential. If the trial function satisfies Poisson's equation and the boundary conditions within the volume in question, the variational technique gives the exact value for the capacitance. The space integral of the Green's function multiplied by the spatial charge distribution does satisfy both the boundary conditions and Poisson's equation, so it can be considered as an optimal trial function. An analytical approach of this nature yields a general expression for the three-dimensional electrostatic capacitance for all geometries, with or without axial symmetry. This can easily be implemented numerically with high accuracy and convergence guaranteed by that of the well-behaved Green's function. Furthermore, knowledge of the charge distributions for a given geometry gives closed-form analytical expressions for the capacitance. Thus, the general formalism was subsequently applied to geometries of interest to the experimentalist. Specific ap-

[1]Present address: Department of Mechanical Engineering, University of Toronto, Toronto, Ont.

[2]Revision received August 25, 1981.

0008-4204/82/020179-17$01.00/0

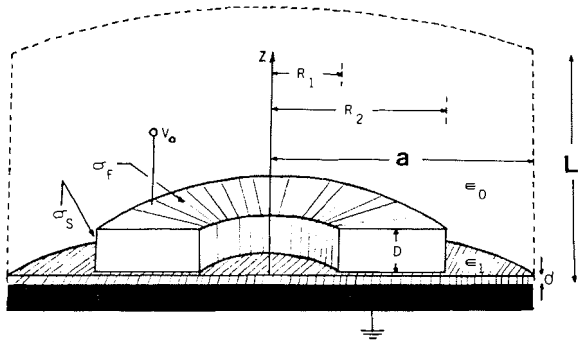

FIG. 1. Cross section of a capacitor with annular plate geometry.

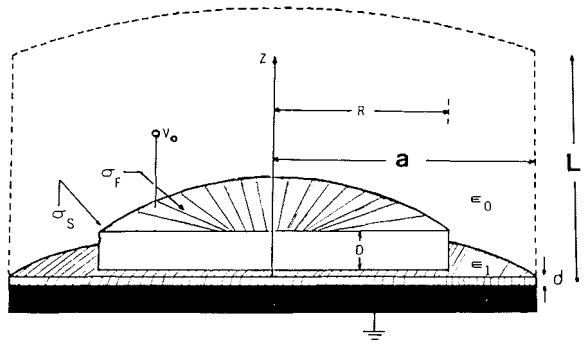

FIG. 2. Cross section of a capacitor with charged disc plate of nonzero thickness.

plications investigated include (*i*) a ring of charge of finite thickness; (*ii*) a disc of finite thickness; and (*iii*) an infinitely thin disc, all raised to a potential V_0 and separated from a grounded plane by a dielectric slab, Figs. 1–3. Each system was assumed to possess cylindrical symmetry, which is the case with a large number of microelectronic configurations. Furthermore, axially symmetric geometries were used in order to simplify the computational task. The resulting mathematical expressions can be compared, in the appropriate limit(s), to well known results for simpler geometries as a further check of the validity of the theory. In the configurations of Figs. 1–3 the radius a of the grounded plate was assumed to be greater than, or equal to, the radius R of the charged plate. The experimentally realistic condition that the grounded substrate thickness, t, be several orders of magnitude larger than those of the charged plate and the dielectric was met by letting $t \rightarrow \infty$. This approximation restricts the domain of the geometry to the semi-infinite space $z \geq 0$. MKS units and cylindrical coordinates were used throughout the present theoretical development.

2. Theory

(1) Capacitance of an arbitrary charge distribution $\sigma(\mathbf{x})$*: variational formulation*

$U[\Psi]$, the total energy of the electric field created as a result of the potential $\Psi(\boldsymbol{x})$ due to an arbitrary charge distribution $\sigma(\boldsymbol{x})$ within a volume V, is given by the expression (7):

$$[1.1] \qquad U[\Psi] = \frac{1}{2} \int_V \sigma(\boldsymbol{x})\Psi(\boldsymbol{x})\, \mathrm{d}^3x$$

The capacitance of the system whose charge distribution $\sigma(\boldsymbol{x})$ causes energy $U[\Psi]$ to be stored in the electric field is (9):

$$[1.2] \qquad C[\Psi] = Q_V^2/2U[\Psi]$$

where Q_V is the total amount of charge in the volume V.

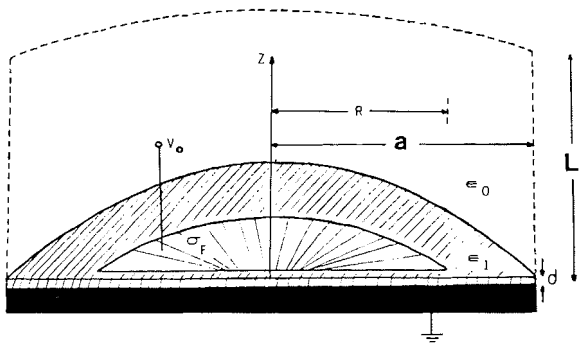

FIG. 3. Cross section of a capacitor with thin charged plate.

Its value can be found by summing up (integrating) the discrete (continuous) charge distribution densities:

$$[1.3] \qquad Q_V = \int_V \sigma(\boldsymbol{x})\, \mathrm{d}^3x$$

In [1.3] the distribution $\sigma(\boldsymbol{x})$ was assumed to be continuous. From [1.1]–[1.3] the electrostatic capacitance $C[\Psi]$ due to the potential distribution $\Psi(\boldsymbol{x})$ can be written:

$$[1.4] \qquad (C[\Psi])^{-1} = \left(\int_V \sigma(\boldsymbol{x})\Psi(\boldsymbol{x})\, \mathrm{d}^3x\right)/\left[\int_V \sigma(\boldsymbol{x})\, \mathrm{d}^3x\right]^2$$

This can be viewed as a variational expression for the capacitance of a charge distribution $\sigma(\boldsymbol{x})$ in a volume V, when the true potential function is not known, but it can be replaced by a trial function $\Psi(\boldsymbol{x})$, which satisfies the boundary conditions on the outer surface(s) of V. [1.4] is a general expression for the electrostatic capacitance and applies to all geometries. It provides upper (or lower) bounds for the true capacitance. If $\Psi(\boldsymbol{x})$ is the true potential function satisfying Poisson's equation within V, then [1.4] gives the true capacitance of the system.

(2) Potential distribution in the semi-infinite space $z \geq 0$

Assuming that the dielectric thin films of the configurations in Figs. 1–3 have a uniform dielectric constant ϵ_1, the potential fields in the positive z half-space are described by the Poisson equation:

$$[2.1a] \quad \nabla^2\Psi(\boldsymbol{x}) = -\sigma_1(\boldsymbol{x})/\epsilon_1; \qquad 0 \le z \le d$$

$$[2.1b] \quad \nabla^2\Psi(\boldsymbol{x}) = -\sigma_2(\boldsymbol{x})/\epsilon_0; \qquad z > d$$

subject to the following boundary conditions:

$$[2.2a] \quad \Psi(\rho,\phi,z = 0) = 0$$

$$[2.2b] \quad \Psi(\rho,\phi,z = L) = 0$$

$$[2.2c] \quad \Psi(\rho = R_1, R_2, R; \phi; z = d, d + D) = V_0$$

In [2.1b] ϵ_0 is the permittivity of free space and z extends throughout the region of space where charges exist. σ_1 and σ_2 are the charge distributions in the dielectric and in the vacuum, respectively. These remain to be determined. The boundary conditions [2.2a,b] impose the requirement that the Green's function $G(\boldsymbol{x},\boldsymbol{x}')$ obey Dirichlet boundary conditions at $z, z' = 0, L$:

$$[2.3] \quad G(\rho,\phi,z = 0, L|\rho',\phi',z' = 0, L) = 0$$

In the (six) boundary conditions [2.2c] the designations $\rho = R_1$, R_2 and $\rho = R$ refer to Fig. 1 and Figs. 2 and 3, respectively.

Green's theorem may be applied to the potential distributions of [2.1a,b] via the use of Green's second identity (7). The result is:

$$[2.4] \quad -\Psi(\boldsymbol{x}) = \int_{V'} G(\boldsymbol{x},\boldsymbol{x}')\nabla^2\Psi(\boldsymbol{x}')\,d^3x' + \int_{S'} \left[G(\boldsymbol{x},\boldsymbol{x}')\frac{\partial}{\partial n'}\Psi(\boldsymbol{x}') - \Psi(\boldsymbol{x}')\frac{\partial}{\partial n'}G(\boldsymbol{x},\boldsymbol{x}')\right] dS'$$
$$= \int_{V'} G(\boldsymbol{x},\boldsymbol{x}')\nabla^2\Psi(\boldsymbol{x}')\,d^3x'$$

because the Dirichlet boundary condition [2.3] implies that $G(\boldsymbol{x},\boldsymbol{x}') = 0$ at all boundaries for $\boldsymbol{x}'$ on the surface S'. The potential distribution $\Psi(\boldsymbol{x}')$ vanishes at $z' = 0$ and $z' = L$, so that the surface integrals in [2.4] are equal to zero. $\partial/\partial n'$ is the normal derivative at the surface S', directed outwards from inside the volume V'.

Form [2.1a,b] and the linearity of the ∇^2 operator, [2.4] becomes:

$$[2.5] \quad \Psi(\boldsymbol{x}) = \frac{1}{\epsilon_1}\int_{V_1'} G(\boldsymbol{x},\boldsymbol{x}')\sigma_1(\boldsymbol{x}')\,d^3x' + \frac{1}{\epsilon_0}\int_{V_2'} G(\boldsymbol{x},\boldsymbol{x}')\sigma_2(\boldsymbol{x}')\,d^3x'$$

where V_1' and V_2' are defined as the space regions $[0,d]$ and $[d,\infty]$, respectively.

For axially symmetric charge distributions about the z-axis the form of the Green's function $G^{(0)}(\boldsymbol{x},\boldsymbol{x}')$ valid for a cylindrical region in the whole $z \ge 0$ half-space with the $z = 0$ plane grounded is (10):

$$[2.6] \quad G^{(0)}(\boldsymbol{x},\boldsymbol{x}') = \frac{1}{\pi a^2}\sum_{n=1}^{\infty} \frac{J_0(k_{0n}\rho)J_0(k_{0n}\rho')\sinh(k_{0n}z_<)\exp(-k_{0n}z_>)}{k_{0n}J_1^2(k_{0n}a)}$$

where a is the radius of the dielectric layer, Figs. 1–3, and $J_m(k_{0n}\rho)$ is the Bessel function of integral order m. The coefficients k_{0n} are related to the nth root, x_{0n}, of the function J_0 in the following manner:

$$[2.7] \quad k_{0n} = x_{0n}/a$$

The variables $z_>$ and $z_<$ are defined as (7):

$$[2.8] \quad z_{\substack{>\\<}} \equiv \begin{Bmatrix}\max\\\min\end{Bmatrix}(z,z')$$

Upon combining the expressions [2.5] and [2.6], the potential distribution in the $z \ge 0$ region can be written in terms of the charge distributions $\sigma_1(\boldsymbol{x})$ and $\sigma_2(\boldsymbol{x})$:

$$[2.9] \quad \Psi(\rho,z) = \frac{2}{\epsilon_1 a^2}\sum_{n=1}^{\infty} \frac{\sinh(k_{0n}z_<)\exp(-k_{0n}z_>)J_0(k_{0n}\rho)}{k_{0n}J_1^2(k_{0n}a)} \int_0^{\infty}\rho'\,d\rho' \int_0^{d} J_0(k_{0n}\rho')\sigma_1(\rho',z')\,dz'$$
$$+ \frac{2}{\epsilon_0 a^2}\sum_{n=1}^{\infty} \frac{\sinh(k_{0n}z_<)\exp(k_{0n}z_>)J_0(k_{0n}\rho)}{k_{0n}J_1^2(k_{0n}a)} \int_0^{\infty}\rho'\,d\rho' \int_d^{\infty} J_0(k_{0n}\rho')\sigma_2(\rho',z')\,dz'$$
$$\equiv \Psi_1(\rho,z) + \Psi_2(\rho,z)$$

In [2.9] the functional forms of $\sigma_1(\rho',z')$ and $\sigma_2(\rho',z')$ depend on the specific axially symmetric shape of the

charged upper plate of the capacitor. Since the expression [2.9] satisfies both the boundary conditions [2.2] and the Poisson's equation [2.1] for all $z \geq 0$, it can be inserted in the variational expression [1.4] to give the *exact* value of the capacitance. The equation [1.4] can be written in cylindrical coordinates as a function of the charge density σ:

$$[2.10] \quad [C(\sigma)]^{-1} = \frac{\int_0^\infty \int_0^\infty \sigma(\rho',z')\Psi[\sigma(\rho',z')]\rho' \, d\rho' \, dz'}{2\pi[\int_0^\infty \int_0^\infty \sigma(\rho',z')\rho' \, d\rho' \, dz']^2}$$

where:

$$\sigma(\rho,z) = \sigma_1(\rho,z) + \sigma_2(\rho,z)$$

(3) Charge distributions for three charged plate geometries

(a) A ring of finite thickness

This upper plate geometry is shown in Fig. 1. The thickness of the right cylindrical ring is D, and the inner and outer radii are R_1 and R_2, respectively. It is assumed that the ring thickness is small in comparison with R_1:

$$[3.1] \quad D \ll R_1 < R_2$$

The condition [3.1] is valid for common experimental configurations in microelectronics applications. Near the edges at $z = d$ and $z = d + D$ the charge density $\sigma_F(\rho)$ on each flat surface of the plate, and that on the cylindrical side surface, $\sigma_S(z)$, become equal and approach that of the charged rectangular wedge (5). The charge in the neighborhood of the wedge is given by (7):

$$[3.2] \quad \sigma_W(x) = \text{const.} \times x^{-1/3}$$

where x is the distance from the edge.

Furthermore, the charge density $\sigma_F(\rho)$ must be a function of R^2 (5), where R is the outward radial distance measured from the inner edge of the ring, Fig. 1: $R_1 \leq R \leq R_2$. The R^2 dependence is dictated by the requirement that $\sigma_F(\rho)$ should be a minimum midway across the surface of the ring, due to the symmetric distribution of charge expected with respect to the (idealized) right-angled outer and inner boundaries of the ring:[3]

$$[3.3] \quad \frac{\partial}{\partial \rho} \sigma_F(\rho) \Big|_{\rho = \frac{1}{2}(R_1 + R_2)} = 0$$

Using a similar argument for the charged side surface of the ring (5), the charge density $\sigma_S(z)$ must be a function of Z^2, where Z is the upward distance measured from the lower edge of the ring. Fig. 1: $d \leq Z \leq d + D$. $\sigma_S(z)$ must have a minimum at the equator:[2]

$$[3.4] \quad \frac{\partial}{\partial z} \sigma_S(z) \Big|_{z = d + (D/2)} = 0$$

Suitable functional forms for σ_F and σ_S, which satisfy the conditions [3.2]–[3.4] are:

$$[3.5] \quad \sigma_F(\rho) = \sum_{n=0}^{\infty} A_n \left\{ 1 - \left[\left(\frac{R_1 + R_2}{2} - \rho \right) \Big/ \left(\frac{R_2 - R_1}{2} \right) \right]^2 \right\}^{n - 1/3}$$

and

$$[3.6] \quad \sigma_S(z) = \sum_{n=0}^{\infty} B_n \left\{ \left(\frac{D}{2R_2} \right)^{2(n - 1/3)} \right\} \left[1 - \left(\frac{d + (D/2) - z}{D/2} \right)^2 \right]^{n - 1/3}$$

The important $n = 0$ term may be called the "fundamental" term in both radial and lateral charge distributions. The remaining terms may be called "correction" terms. This nomenclature has been used previously by Smythe (5) in his treatment of the charge densities on the surfaces of charged right circular cylinders. Use of the condition [3.1] shows that only the fundamental term $n = 0$ in [3.6] contributes significantly to the value of the charge density anywhere on the side of the ring, and therefore it is the only term that will be kept in what follows. Similarly, in his treatment of the numerical values of the coefficients of the radial charge density function $\sigma_F(\rho)$

[3]In reality the right-angled boundaries of the conducting cylinder are not infinitely sharp. The finite radius of curvature would add a correction term to the equations for $\sigma_W(x)$. In the limit of the geometries of Figs. 1 and 2, i.e., for $D \gg r_c$, this term is negligible; r_c is the radius of curvature of a rounded edge.

for different (D/R_2) ratios of the right charged cylinder, Smythe has shown that only the fundamental term is important. The coefficients of the correction terms decrease rapidly, especially for $D \ll R_2$ values. Therefore, only the fundamental term will be kept in [3.5] without loss of precision. The expressions [3.5] and [3.6] are then simplified to:

$$[3.7] \quad \sigma_F(\rho) = \frac{c_1}{\left\{1 - \left[\left(\frac{R_1 + R_2}{2} - \rho\right)\Big/\left(\frac{R_2 - R_1}{2}\right)\right]^2\right\}^{1/3}}$$

and

$$[3.8] \quad \sigma_S(z) = \frac{c_2}{\left\{1 - \left[\left(d + \frac{D}{2} - z\right)\Big/(D/2)\right]^2\right\}^{1/3}}$$

where: $c_1 \equiv A_0$ and $c_2 \equiv B_0(D/2R_2)^{-2/3}$. In order that these fundamental terms match at the edges, it is necessary to impose the requirements:

$$[3.9] \quad \lim_{\epsilon \to 0} \sigma_F(R_1 + \epsilon) = \lim_{\epsilon \to 0} \sigma_F(R_2 - \epsilon) = \lim_{\epsilon \to 0} \sigma_S(D + d - \epsilon) = \lim_{\epsilon \to 0} \sigma_S(d + \epsilon)$$

Keeping terms of only first order in $\epsilon \ll 1$, we find:

$$[3.10] \quad c_2 = c_1\left[\frac{2(R_2 - R_1)}{D}\right]^{1/3}$$

Collecting terms yields the charge density on the cylindrical conducting ring in the symbolic form:

$$[3.11] \quad \sigma(\rho,z) = \sigma_F(\rho) + \sigma_S(z) = c_1 \left\{ \frac{[H(\rho - R_1) - H(\rho - R_2)][\delta(z - d) + \delta(z - d - D)]}{\left(1 - \left[\left(\frac{R_1 + R_2}{2} - \rho\right)\Big/\left(\frac{R_2 - R_1}{2}\right)\right]^2\right)^{1/3}} \right.$$

$$\left. + \frac{[H(z - d) - H(z - d - D)][\delta(\rho - R_1) + \delta(\rho - R_2)]}{\left(\frac{D}{2(R_2 - R_1)}\right)^{1/3}\left(1 - \left[\left(d + \frac{D}{2} - z\right)\Big/(D/2)\right]^2\right)^{1/3}} \right\}$$

In the expression [3.11] the function H is the Heaviside operator, defined as:

$$[3.12] \quad H(x) = \begin{cases} 0; & x < 0 \\ 1; & x > 0 \end{cases}$$

The actual value of c_1 in [3.11] is a function of the applied voltage V_0. However, it is of no importance in the calculation of the capacitance. The latter is given as the ratio of two expressions, both of which are proportional to c_1^2.

(b) A disc of nonzero thickness

For this configuration the radial charge distribution equation [3.7] must be modified, in order to dispose of the nonphysical charge density singularity along the z-axis at the pole. For this geometry $\sigma_F(\rho)$ on the two flat surfaces must be a function of ρ^2 and have a minimum at the center, due to the symmetric charge distribution:

$$[3.13] \quad \frac{\partial}{\partial \rho}\sigma_F(\rho)\big|_{\rho=0} = 0$$

An expression satisfying the condition [3.13] has been given by Smythe (5). Using the constraint:

$$[3.14] \quad D \ll R$$

the functional form of the radial charge distribution can be derived in a manner entirely analogous to that used to derive [3.7].

It is easy to verify that [3.8] is also valid in this case and gives the correct lateral charge distribution. Collecting terms yields the charge density on the cylindrical conducting disc in the symbolic form:

$$[3.15]\quad \sigma(\rho,z) = \sigma_F(\rho) + \sigma_S(z) = c_1(V_0)\left\{\frac{[H(\rho) - H(\rho - R)][\delta(z - d) + \delta(z - d - D)]}{[1 - (\rho/R)^2]^{1/3}} + \frac{[H(z - d) - H(z - d - D)]\delta(\rho - R)}{(D/2R)^{1/3}\left(1 - \left[\left(d + \frac{D}{2} - z\right)\Big/(D/2)\right]^2\right)^{1/3}}\right\}$$

(c) An infinitely thin disc

For a conducting disc with zero thickness [3.2] can be changed to (7):

$$[3.16]\quad \sigma_W(x) = \text{const.} \times x^{-1/2}$$

By combining the condition [3.16] with the radial condition [3.13], the charge distribution density may be written in the symbolic form:

$$[3.17]\quad \sigma(\rho,z) = \sigma_F(\rho,z) = c_1(V_0)\left\{\frac{[H(\rho) - H(\rho - R)]\,\delta(z - d)}{[1 - (\rho/R)^2]^{1/2}}\right\}$$
$$\sigma_S(z) = 0$$

The charge densities $\sigma_1(\boldsymbol{x})$ and $\sigma_2(\boldsymbol{x})$ in [2.1] and [2.9] can be defined in terms of $\sigma_F(\rho)$ and $\sigma_S(z)$:

$$[3.18]\quad \sigma_1(\rho,z) = \frac{1}{2}\sigma_F(\rho)$$

$$[3.19]\quad \sigma_2(\rho,z) = \frac{1}{2}\sigma_F(\rho) + \sigma_S(z)$$

In [3.18] and [3.19] it is assumed that the charge density associated with the dielectric is that of the lower flat surface of the upper conducting plate. The charge density associated with the vacuum is that of the upper flat surface of the charged plate and of the cylindrical side surface.

When the expressions for σ_1 and σ_2 from [3.18] [3.19], [3.11], [3.15], and [3.17] are inserted in the integrand of the $\Psi(\rho,z)$, [2.9], the potentials Ψ_1 and Ψ_2 satisfy for all three geometries the relationship:

$$[3.20]\quad \epsilon_1 \frac{\partial}{\partial z}\Psi_1(\rho,z)\big|_{z=d} = \epsilon_0 \frac{\partial}{\partial z}\Psi_2(\rho,z)\big|_{z=d}$$

The equation [3.20] indicates that the continuity condition for the normal component of the displacement vector $\boldsymbol{D}_i = -\epsilon_i \nabla \Psi_i$ is valid outside the upper plate area, at the vacuum–dielectric interface, where the free charge density is zero, as expected.

3. Special cases

Substitution of the expression [2.9] for the electrostatic potential into [2.10], using [3.18] and [3.19], gives a general and exact expression for the capacitance of the configurations in Figs. 1–3:

$$[4.1]\quad [C(\sigma_F,\sigma_S)]^{-1} = \frac{1}{\pi a^2}\sum_{n=1}^{\infty}\left\{\frac{\left[\int_0^\infty\int_0^\infty\left\{J_0(k_{0n}\rho')\left[\frac{1}{2}\left(\frac{1}{\epsilon_1} + \frac{1}{\epsilon_0}\right)\sigma_F(\rho') + \frac{1}{\epsilon_0}\sigma_S(z')\right]\right\}\rho'\,d\rho'\,dz'\right]}{k_{0n}J_1^2(k_{0n}a)\left[\int_0^\infty\int_0^\infty\left\{\sigma_F(\rho') + \sigma_S(z')\right\}\rho'\,d\rho'\,dz'\right]^2}\right.$$
$$\left.\times\left[\int_0^\infty\int_0^\infty\left\{J_0(k_{0n}\rho')[\sigma_F(\rho') + \sigma_S(z')]\sinh(k_{0n}z')\exp[-k_{0n}(d + D)]\right\}\rho'\,d\rho'\,dz'\right]\right\}$$

This may be written more compactly in the form:

$$[4.2]\quad C^{-1} = \frac{1}{\pi a^2}\sum_{n=1}^{\infty}\left[\frac{\exp[-k_{0n}(d + D)]}{k_{0n}J_1^2(k_{0n}a)}\right]\frac{Q_2(k_{0n};R_1,R_2,D)\,Q_3(k_{0n};R_1,R_2,d,D)}{[Q_1(R_1,R_2,D)]^2}$$

where:

[4.3a] $Q_1 = \int_0^\infty \rho\, d\rho \int_0^\infty dz\, [\sigma_F(\rho) + \sigma_S(z)]$

[4.3b] $Q_2 = \int_0^\infty \rho\, d\rho \int_0^\infty dz\, J_0(k_{0n}\rho)\left[\frac{1}{2}\left(\frac{1}{\epsilon_1} + \frac{1}{\epsilon_0}\right)\sigma_F(\rho) + \frac{1}{\epsilon_0}\sigma_S(z)\right]$

[4.3c] $Q_3 = \int_0^\infty \rho\, d\rho \int_0^\infty dz\, J_0(k_{0n}\rho)\, [\sigma_F(\rho) + \sigma_S(z)]\, \sinh\,(k_{0n}z)$

The integrals [4.3] may be evaluated for each of the three geometries by using (*a*) [3.11] for the annular upper plate; (*b*) [3.15] for the disc with nonzero thickness; and (*c*) [3.17] for the infinitely thin disc. These evaluations appear in the Appendices I–III.

A variety of interesting special cases will be investigated below:

(*i*) The expression obtained for the infinitely thin disc upon substitution of [C.1]–[C.3] into [4.2] and using [3.17] is:

[4.4] $$[C(a,R,d)]^{-1} = \left(\frac{1}{2\epsilon_1\pi a^2}\right) \sum_{n=1}^{\infty} \left(\frac{1 - \exp\,(-2k_{0n}d)}{k_{0n}J_1^2(k_{0n}a)}\right) \frac{\left[\int_0^R J_0(k_{0n}\rho)\sigma(\rho)\rho\, d\rho\right]^2}{\left[\int_0^R \sigma(\rho)\rho\, d\rho\right]^2}$$

$$= \left(\frac{1}{2\epsilon_1\pi a^2R^2}\right) \sum_{n=1}^{\infty} \left[\frac{1 - \exp(-2k_{0n}d)}{k_{0n}^3 J_1^2(k_{0n}a)}\right] \sin^2\,(k_{0n}R)$$

The following limits may be easily obtained from [4.4]

(*i*.1) In the limit of an infinitely large grounded conductor, $a \to \infty$. In this limit the discrete variable k_{0n} becomes continuous. The formalism developed so far using finite values of the radius a may be carried over to the case $a \to \infty$, upon transforming (7):

[4.5] $$\frac{\sqrt{2}}{aJ_1(k_{0n}a)} \to k$$

and

[4.6] $$\frac{2}{a^2} \sum_{n=1}^{\infty} \frac{1}{[J_1(k_{0n}a)]^2} \to \int_0^\infty k\, dk$$

Under the transformation rule [4.5] and [4.6], [4.4] becomes:

[4.7] $$[C(R,d)]^{-1} = \frac{1}{4\pi\epsilon_1} \int_0^\infty dk \left\{[1 - \exp\,(-2kd)] \frac{\left[\int_0^R J_0(k\rho)\sigma(\rho)\rho\, d\rho\right]^2}{\left[\int_0^R \sigma(\rho)\rho\, d\rho\right]^2}\right\}$$

The expression [4.7] gives the capacitance of a flat, thin, circular disc of radius R located parallel to, and a distance d above, an infinitely large grounded conducting plane. The in-between space is assumed to be filled with a dielectric having dielectric constant ϵ_1. This expression is identical to that presented by Jackson (7). It was derived here as a limit of more general considerations. Equation [4.7] may be integrated in closed form with the aid of ref. 13, entry 3.915.4, using the exact charge distribution [3.17]. The result is:

[4.8] $$C(R,d) = \frac{4\pi\epsilon_1 R}{\frac{\pi}{2} - \cot^{-1}\,(d/R) - (d/2R)\,\ln\left(\frac{(d/R)^2}{1 + (d/R)^2}\right)}$$

for $d \gg R$, $\cot^{-1}\,(d/R) \to 0$, and $\ln\,[(d/R)^2/(1 + (d/R)^2)] \sim 0$. In this limit:

[4.9] $$C(R,d) \sim 8\epsilon_1 R$$

in agreement with the exact capacitance value of an isolated charged disc in a dielectric of constant ϵ_1.

(*i*.2) If the integrations of [4.4] are performed with the incorrect but popular assumption that $\sigma(\rho)$ = constant, the resulting expression is:

[4.10] $$C^{-1} = \left(\frac{2}{\pi\epsilon_1 a^2R^2}\right) \sum_{n=1}^{\infty} \left[\frac{1 - \exp\,(-2k_{0n}d)}{k_{0n}^3}\right] \left\{\frac{J_1(k_{0n}R)}{J_1(k_{0n}a)}\right\}^2$$

Assuming further that (*i*) $d \ll R$ and (*ii*) $R = a$, [4.10] reduces to:

$$[4.11] \quad C^{-1} \simeq \left(\frac{4d}{\pi\epsilon_1 R^4}\right) \sum_{n=1}^{\infty} (1/k_{0n})^2$$

The orthonormality property of the complete set of functions used for the Green's function expansion yields the sum-rule:

$$[4.12] \quad \sum_{n=1}^{\infty} (1/k_{0n})^2 = R^2/4$$

From [4.11] and [4.12] we obtain:

$$[4.13] \quad C = \epsilon_1 \frac{\pi R^2}{d}$$

which is the result expected for the capacitance between two plates of equal radii R, which are uniformly charged and separated by a distance $d \ll R$, so that charge accumulation at the edges will not affect the value of C.

(*ii*.1) If the charge density is assumed constant in the geometry of Fig. 1, the capacitance of this configuration is given by [4.1] upon setting:

$$[4.14] \quad \sigma_F = \sigma_S = \sigma \text{ (independent of } \rho, z)$$

Then the integrations over ρ and z become trivial, and [4.1] reduces to the expression:

$$[4.15] \quad C^{-1} = \left(\frac{1}{2\pi\epsilon_{\text{eff}} a^2 (R_2^2 - R_1^2)}\right) \left\{ \sum_{n=1}^{\infty} \left(\frac{1 + \exp(-k_{0n}D) - \exp[-k_{0n}(2d + D)] - \exp[-2k_{0n}(d + D)]}{k_{0n}^3 J_1(k_{0n}a)} \right) \times [R_2 J_1(k_{0n}R_2) - R_1 J_1(k_{0n}R_1)]^2 \right\}$$

where:

$$[4.16] \quad \frac{1}{\epsilon_{\text{eff}}} \equiv (1/2)\left(\frac{1}{\epsilon_1} + \frac{1}{\epsilon_0}\right) + \frac{1}{\epsilon_0}$$

The equation [4.15] gives the capacitance of the structure of Fig. 1 with a uniformly charged annular upper plate. It does not reflect the true charge distribution; however, it has been included because it adds insight to the way the various geometric quantities of Fig. 1 contribute to the total capacitance of the system.

(*ii*.2) Upon setting $R_1 = 0$ in [4.15], the capacitance of the structure of Fig. 2 is obtained, assuming that the upper plate is uniformly charged:

$$[4.17] \quad C^{-1} = \frac{1}{2\pi\epsilon_{\text{eff}} a^2 R^2} \sum_{n=1}^{\infty} \left(\frac{1 + \exp(-k_{0n}D) - \exp[-k_{0n}(2d + D) - \exp[-2k_{0n}(d + D)]}{k_{0n}^3} \right) \left[\frac{J_1(k_{0n}R)}{J_1(k_{0n}a)}\right]^2$$

If we set $D = 0$ and $\epsilon_1 = \epsilon_0$ in [4.17] we obtain [4.10], which corresponds to the two-dimensional, thin, uniformly charged disc geometry of Fig. 3.

(*ii*.3) Upon setting $a = R$ and (d/R), $(D/R) \ll 1$, [4.17] reduces to:

$$[4.18] \quad C^{-1} = \frac{2d + D}{\pi\epsilon_{\text{eff}} R^4} \sum_{n=1}^{\infty} (1/k_{0n})^2$$

Using the sum-rule [4.12] in [4.18] yields:

$$[4.19] \quad C^{-1} = \frac{2d + D}{4\pi\epsilon_{\text{eff}} R^2}$$

Defining:

$$[4.20] \quad C_A \equiv (2\epsilon_{\text{eff}}) \frac{\pi R^2}{d}$$

and

$$[4.21] \quad C_B \equiv (2\epsilon_{eff}) \frac{\pi R^2}{(D/2)}$$

[4.18] may be written in the form:

$$[4.22] \quad \frac{1}{C} = \frac{1}{C_A} + \frac{1}{C_B}$$

The equation [4.22] shows that in the limit of two capacitor plates of equal areas, the measured capacitance is equivalent to that of two capacitors connected in series in a medium with dielectric constant given by twice the effective constant ϵ_{eff}. One of these capacitors, C_A, has plate separation d, and the other, C_B, has plate separation $D/2$. This latter separation may be understood by considering the symmetry of the geometry of the cylindrical upper plate, as well as the assumed uniform distribution of charge over its surface. The average position of the charge on the cylinder is given by:

$$[4.23] \quad \langle x \rangle = \frac{\int_d^{d+D} x\sigma \, dx}{\int_d^{d+D} \sigma \, dx} = d + \frac{D}{2}$$

i.e., $\langle x \rangle$ is symmetrically located in the equator of the cylinder, which acts as the effective position of the charge.

(*ii*.4) If, instead of the two media with dielectric constants ϵ_0, ϵ_1, one uniform medium is present with $\epsilon_1 = \epsilon_0$, then the definition [4.16] gives:

$$\epsilon_{eff} = \frac{1}{2}\epsilon_0$$

Equation [4.19] can then be written:

$$[4.24] \quad C = \epsilon_0 \frac{\pi R^2}{\left(d + \frac{D}{2}\right)} = \epsilon_0 \frac{\pi R^2}{\langle x \rangle}$$

Equation [4.24] shows that in the limit of a uniform dielectric medium the two series capacitors may be replaced by one with plate separation equal to the average charge position $\langle x \rangle$, as expected.

(*ii*.5) In the geometry of Fig. 1, using $a = R_2$ and (d/R_2), $(D/R_2) \ll 1$, [4.15] reduces to:

$$[4.25] \quad C^{-1} = \left[\frac{2d + D}{\pi\epsilon_{eff}(R_2^2 - R_1^2)^2}\right] \sum_{n=1}^{\infty} \left(\frac{1}{k_{0n}}\right)^2 \left[1 - \left(\frac{R_1}{R_2}\right) \frac{J_1(k_{0n}R_1)}{J_1(k_{0n}R_2)}\right]^2$$

In the limit of $D = 0$, [4.25] gives the capacitance between two circular plates of radius R_2, a distance d apart and when the upper plate has a circular hole of radius R_1 in the middle and is charged uniformly:

$$[4.26] \quad C(D = 0, \epsilon_1 = \epsilon_0) = \epsilon_0 \frac{A_{eff}(R_1)}{d}$$

where

$$A_{eff}(R_1) \equiv \frac{\pi(R_2^2 - R_1^2)}{4 \sum_{n=0}^{\infty} \frac{1}{k_{0n}^2(R_2^2 - R_1^2)} \left[1 - \left(\frac{R_1}{R_2}\right) \frac{J_1(k_{0n}R_1)}{J_1(k_{0n}R_2)}\right]^2}$$

In the limit $R_1 = 0$, it is easy to show that: $A_{eff}(0) = \pi R_2^2$ = area of a disc of radius R_2 as expected.

4. Discussion

Numerical computations of the expression [4.2] have been performed using the expressions for Q_1, Q_2, and Q_3 from the Appendices I–III. It was found that the infinite summation over n could be approximated adequately by using a trunkation at $n \leq 400$, so that the results varied with n by less than 0.1%. Rapid convergence was achieved using both the Taylor series and the asymptotic expansions in the appropriate limits for the Bessel and the modified

Bessel functions of the various orders:

$$[5.1]\quad J_p(x) = \begin{cases} \displaystyle\sum_{k=0}^{\infty} \frac{(-1)^k}{k!\,\Gamma(p+k+1)}\,(x/2)^{2k+p} & \text{(Taylor)} \\ \sqrt{2/\pi x}\,\cos\left(x - \frac{\pi}{2}p - \frac{\pi}{4}\right) & \text{(Asymptotic)} \end{cases}$$

$$[5.2]\quad I_p(x) = \begin{cases} \displaystyle\sum_{k=0}^{\infty} \frac{1}{k!\,\Gamma(p+k+1)}\,(x/2)^{2k+p} & \text{(Taylor)} \\ \dfrac{e^x}{\sqrt{2\pi x}} \displaystyle\sum_{k=0}^{\infty} \frac{(-1)^k}{(2x)^k} \frac{\Gamma\left(p+k+\frac{1}{2}\right)}{k!\,\Gamma\left(p-k+\frac{1}{2}\right)} & \text{(Asymptotic)} \end{cases}$$

Using a minimization routine to calculate the difference of the numerical values of the asymptotic and the Taylor expansions in the series [5.1], [5.2] it was found that the transition from the Taylor series to the asymptotic limit occurs at $x_0 = 4 \pm 0.1$ for both $J_p(x)$ and $I_p(x)$. The actual value of x_0 varies slightly with p. The values of both $J_p(x)$ and $I_p(x)$ are effectively independent of k for $k \geq 25$. This was taken as the cutoff term for both series in all computer calculations.

For the purposes of the charged ring calculations, the value of $A_m(x)$, [A.12], was only required for $x < 1$. In this limit [A.12] may be expressed in closed form as:

$$[5.3]\quad A_m(x) = \frac{1}{2}\,\Gamma(2/3) \sum_{k=0}^{\infty} \frac{(-1)^k}{k!\,\Gamma(m+k+1)} \frac{\Gamma\left(k+\frac{m+1}{2}\right)}{\Gamma\left(k+\frac{m}{2}+\frac{7}{6}\right)}\,(x/2)^{2k+m}$$

Numerical results for an infinitely thin charged disc at a distance d above an infinite grounded plane are shown in Fig. 4 (from [4.8]). As seen in Fig. 4*a*, the capacitance of the system decreases with increasing d. For values of $d > 1$ mm the system is essentially an isolated charged thin disc, and the capacitance saturates at the value $8\epsilon_1 R$, as expected. Figure 4*b* is a plot of the capacitance of the system as a function of the radius R of the charged disc. Although the R dependence of [4.8] is complicated, a monotonic increase of the capacitance due to the increased area of the upper plate is to be expected, provided that the area of the grounded plate is always larger than that of the charged plate. This condition is always satisfied in the limit in which [4.8] is valid, i.e., $a \to \infty$. When the grounded plate has a finite radius, the critical factor upon which the capacitance of the system depends is the spatial charge distribution on the charged upper plate. For an infinitely thin charged disc the charge tends to accumulate at the circular rim, away from the center. This is indicated by the (integrable) infinity at $\rho = R$ in the expression [3.17] for the charge density $\sigma(\rho,z)$. This charge behavior causes fringing of the lines of force at locations close to, or at, the rim. If the areas of both plates are the same, all the lines of force must be distributed between points on the rim of the upper plate and corresponding points on the rim of the grounded plate. If the area of one of the plates increases, the number of lines of force within an area equal to the projection of the smaller plate onto the larger one decreases, as some of these lines are distributed at locations outside the projected area. This simple argument shows that when both plates have the same area all of the charge contributes to the value of the capacitance. When unequal areas are involved some charge is distributed outside the region between the smaller plate and its projection onto the larger plate. This charge does not contribute as effectively to the value of the capacitance. It is therefore expected that the capacitance of the configuration in Fig. 3 will decrease when the plate areas are unequal. Figure 5 is a plot of the capacitance as a function of the grounded plate radius, a, with the interplate distance d as a parameter. Both curves are normalized with respect to the value of the capacitance for identical plates with radii equal to 625 μm. The capacitance of the configuration with $d =$ 0.01 μm decreases rapidly with increasing grounded plate radius and it saturates at ca. 85% of the initial value for $a \geq 625.05$ μm. For larger grounded plate radii no significant redistribution of the charge between the two plates will occur. Owing to the narrow gap

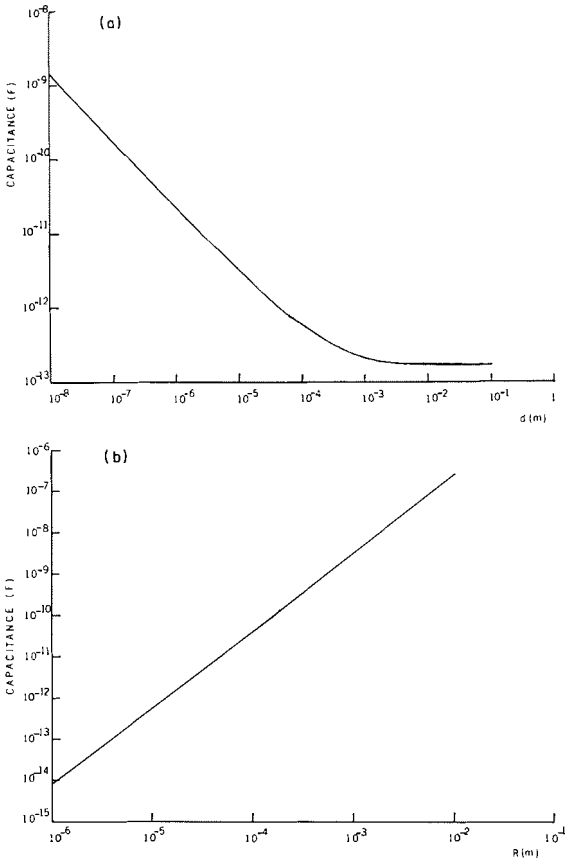

FIG. 4. (*a*) Capacitance of an infinitely thin disc vs. interplate distance with $R = 625$ μm, $C_\infty = 1.725 \times 10^{13}$ F, and $a = \infty$. (*b*) Capacitance of an infinitely thin disc vs. charged plate radius ($a = \infty$).

between the plates, the system with $a \geq 625.05$ μm behaves like a charged disc above an infinite grounded plate, with a capacitance given by [4.8]. Computer simulations have shown that the geometric criterion for the capacitance to assume the limiting value of [4.8] is:

$$[5.4] \quad \Delta R \sim 10d$$

where:

$$\Delta R = |a - R|$$

The capacitance of the $d = 1$ μm configuration decreases much more gradually with increasing lower plate radius. Due to the relatively large distance between the two plates, the effect of the charge redistribution is not significant, unless relatively large lower plate areas are involved. As a result, the asymptotic value of $8\epsilon_1 R$ occurs for $\Delta R \sim 10$ μm, in agreement with the criterion [5.4]. It is evident from Fig. 5 that an approximately 15% reduction of the calculated value is the maximum correction to the capacitance required when the expression [4.13] is used for unequal area

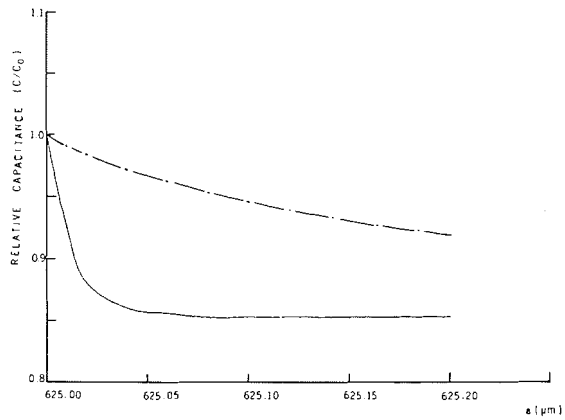

FIG. 5. Capacitance of an infinitely thin disc vs. ground plate radius for $R = 625$ μm and $d = 0.01$ μm (——), $d = 1$ μm (—·—·—).

plates. This maximum correction is needed for measurements of thin oxide layers on the order of 0.01–0.1 μm thickness. The sensitivity of the value of the capacitance to minute changes in plate radius can be understood mathematically from the fact that the electrostatic capacitance is an integral over the charge distribution, which has a pole at $\rho = R$, i.e., at the edge of the plates. Small variations in the plate dimension(s) can change the value of the integral significantly, as most of the contribution is due to the inclusion of the point $\rho = R$ in the active capacitor area. If the charge were distributed uniformly, [4.13] indicates that $C_1/C_0 = (R_1/R_0)^2 \simeq 1$ for all $R_1 \leq 1.04R_0$. As expected, the value for the capacitance is much less sensitive to small plate area differences in this case.

The effect of a charged plate of finite thickness on the measured value of the capacitance has been described by [4.22] for the case of a uniform charge distribution. Figure 6*a* is a plot of the general case, using [4.2] and the charge distribution [3.11]. It may be observed that an increase from 0.1 to 1 μm in upper plate thickness D decreases the effective value of the capacitance by one order of magnitude. This occurs because contributions made by charges from the upper surface of the top plate to the capacitance integral become less important with increasing thickness, i.e., with increasing distance of this surface from the grounded plate. As the interplate distance d increases, the difference in height between the upper and lower surfaces of the charged plate decreases in importance for the value of the capacitance. For values such that $d \gtrsim 10D$, the charged plate behaves like an infinitely thin disc and the capacitance value approaches asymptotically that of an isolated disc. Figure 6*b* is a plot of the capacitance as a function of the charged plate thickness, with the grounded plate radius a as a parameter. For thin charged

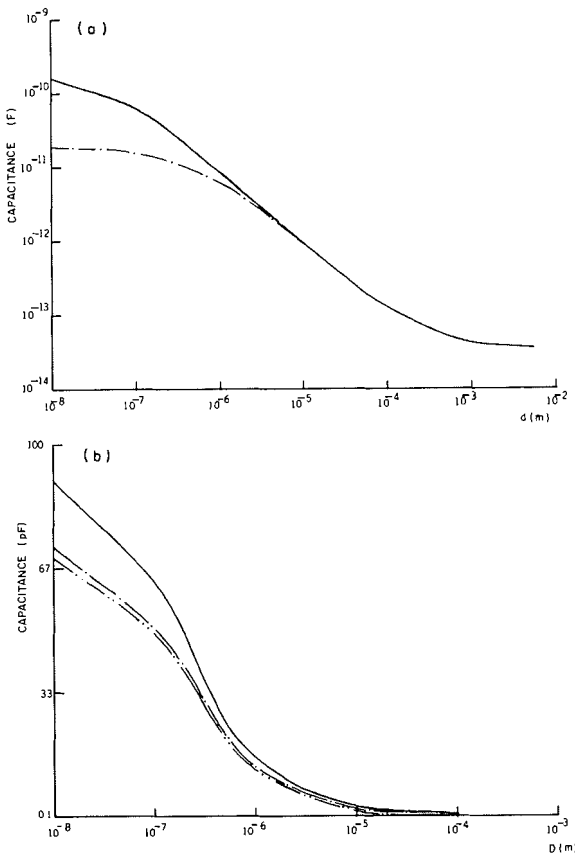

FIG. 6. (*a*) Capacitance of a disc vs. interplate distance for $a = R = 625$ μm and $D = 0.1$ μm (——), $D = 1.0$ μm (—·—·—). (*b*) Capacitance of a disc above a finite ground plane for $a = 100R$ (——), $a = 10R$ (—·—·—), and $a = R$ (—· ·—· ·—).

plates the decrease in capacitance with increasing a is significant, as expected for $d \leq a$ (compare with Fig. 5). For $a \gg R$ the configuration of an infinitely thin charged disc above an infinite grounded plane is approached and the curves become less sensitive to the value of a. However, an increase in the thickness D brings about a reduction in the capacitance, as discussed in connection with Fig. 6*a*. For $D \gg d$, only the charge in the lower flat surface and the adjacent cylindrical sides contribute to the value of the capacitance. In this limit the capacitance is a function of the grounded plate radius only, and all three curves approach values determined by the line-of-force distribution in the available grounded plate area.

When the charged plate has the ring shape of Fig. 1, the capacitance is expected to decrease for values of the inner radius R_1 close to that of the outer radius R_2, because the total charged area decreases. Figure 7 is a plot of [4.2] with Q_i values from Appendix I, having the

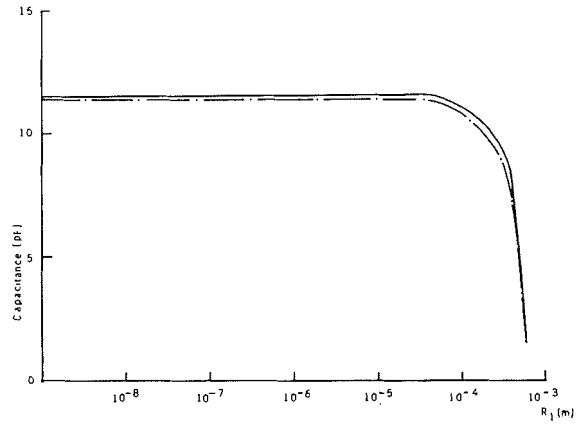

FIG. 7. Capacitance of an annulus above a finite ground plane with $a = 625$ μm, $d = 0.1$ μm, and $D = 1$ μm. (——) is for $a = R_2$; (—·—·—) for $a = 100R_2$.

grounded plate radius a as a parameter. The value of the capacitance is essentially independent of R_1 for values of $R_1 \lesssim 0.1R_2$. A rapid decrease in the value of $C(R_1, R_2)$ is observed for $R_1 > 200$ μm and it results in $C = 0$ for $R_1 = R_2$. Figure 7 indicates that the difference in the values of C between the $a = R_2$ and the $a = 100R_2$ configurations is smaller than that between the respective configurations of a charged disc with $a = R$ and $a = 100R$, Fig. 6*b*. This is the result of charge accumulation at the inner edges of the ring, which contributes significantly to the value of the capacitance, as opposed to contributions from the relatively charge-depleted disc center. This inner charge accumulation is just as important to the determination of the capacitance value as the outer edge charge distribution. Therefore, small differences between the radii a and R_2 are not so important in determining C for the ring structure as differences between a and R are for the disc. In mathematical terms, the annular structure charge distribution has two poles at $\rho = R_1$ and $\rho = R_2$, whereas the disc has only one at $\rho = R$. The integrals for C depend on contributions from these poles. In the disc case the capacitance is sensitive to plate radius values in the range $a \sim R$, while in the annular case the large added contribution from the $\rho = R_1$ pole decreases the sensitivity of the C value dependence to contributions from the $a \sim R_2$ pole.

5. Conclusions

The present variational–Green's function formalism for the determination of the capacitance of complex three-dimensional geometries has been shown to give general and exact expressions for the capacitance, regardless of the specific geometrical parameters. Use of physically realistic charge distributions yielded closed

form expressions for geometries of interest to the experimentalist. It was shown that C is sensitive to the thickness and other dimensions of the capacitor plates, as well as to the spatial charge distribution. Numerical calculations indicated that care must be taken in interpreting capacitance measurements when using simplified formulae such as [4.13], which might give inaccuracies greater than 10%.

1. G. KIRCHOFF. Monatsber. Dtsch. Akad. Wiss. Berlin, 144 (1877).
2. J. C. COOKE. Z. Angew. Math. Mech. **38**, 349 (1958).
3. M. SHIMASAKI and T. KIYONO. Electron. Commun. Jpn. B, **54**, 80 (1971).
4. D. KIRKHAM. J. Appl. Phys. **28**, 724 (1957).
5. W. R. SMYTHE. J. Appl. Phys. **27**, 917 (1956).
6. R. E. COLLIN. *In* Field theory of guided waves. McGraw-Hill, New York, NY. 1960. p. 162.
7. J. D. JACKSON. *In* Classical electrodynamics. 2nd ed. J. Wiley Interscience, New York, NY. 1975.
8. W. C. CHEW and J. A. KONG. J. Math. Phys. In press.
9. G. E. OWEN. *In* Electromagnetic theory. Allyn and Bacon Inc., Boston, MA. 1963.
10. W. R. SMYTHE. *In* Static and dynamic electricity. McGraw-Hill, New York, NY. 1950.
11. I. M. RYSHIK and I. S. GRADSTEIN. *In* Tables of series, products, and integrals. Deutscher Verlag der Wissenschaften, Berlin, W. Germany. 1963.
12. D. L. KREIDER, R. G. KULLER, and R. D. OSTBERG. *In* Elementary differential equations. Addison-Wesley, New York, NY. 1968. Chapt. 7.
13. I. M. RYSHIK and I. S. GRADSTEIN. *In* Table of integrals, series, and products. 4th ed. Academic Press, New York, NY. 1965.

Appendix I

Evaluation of the integrals Q_1, Q_2, Q_3 *for the charged annulus*

(*i*) $Q_1 = \int_0^\infty \rho\, d\rho \int_0^\infty dz\, [\sigma_F(\rho) + \sigma_S(z)]$

Using the expression [3.11], the definition of the Heaviside operator, and the properties of the delta function we can write:

$$[A.1]\quad Q_1 = c_1 \left\{ 2 \int_{R_1}^{R_2} \left(\frac{\rho\, d\rho}{\left\{ 1 - \left[\left(\frac{R_1 + R_2}{2} - \rho \right) \Big/ \left(\frac{R_2 - R_1}{2} \right) \right]^2 \right\}^{1/3}} \right) + \left(\frac{2(R_2 - R_1)}{D} \right)^{1/3} \times (R_1 + R_2) \int_d^{d+D} \left(\frac{dz}{\left\{ 1 - \left[\left(d + \frac{D}{2} - z \right) \Big/ (D/2) \right]^2 \right\}^{1/3}} \right) \right\}$$

Using obvious transformations Q_1 becomes:

$$[A.2]\quad Q_1 = c_1 \left\{ (R_2^2 - R_1^2) \int_0^{\pi/2} \cos^{1/3} x\, dx + [2(R_2 - R_1)D^2]^{1/3} (R_1 + R_2) \int_0^{\pi/2} \cos^{1/3} x\, dx \right\}$$

Using ref. 11, entry 3.421.2, we find:

$$[A.3]\quad \int_0^{\pi/2} \cos^{1/3} x\, dx = \frac{[\Gamma(2/3)]^2}{2^{2/3}\Gamma(4/3)}$$

Therefore:

$$[A.4]\quad Q_1(R_1,R_2,D) = c_1 \frac{[\Gamma(2/3)]^2}{2^{2/3}\Gamma(4/3)} \left\{ (R_2^2 - R_1^2) + (R_1 + R_2)[2(R_2 - R_1)D^2]^{1/3} \right\}$$

(*ii*) $Q_2 = \int_0^\infty \rho\, d\rho \int_0^\infty dz\, J_0(k_{0n}\rho) \left\{ \frac{1}{2}(\epsilon_1^{-1} + \epsilon_0^{-1})\, \sigma_F(\rho) + \epsilon_0^{-1} \sigma_S(z) \right\}$

From [3.11] we can write:

$$[A.5]\quad Q_2 = c_1 \left\{ (\epsilon_1^{-1} + \epsilon_0^{-1}) \int_{R_1}^{R_2} \left[\frac{\rho J_0(k_{0n}\rho)\, d\rho}{\left\{ 1 - \left[\left(\frac{R_1 + R_2}{2} - \rho \right) \Big/ \left(\frac{R_2 - R_1}{2} \right) \right]^2 \right\}^{1/3}} \right] + \epsilon_0^{-1} \left(\frac{2(R_2 - R_1)}{D} \right)^{1/3} \times [R_1 J_0(k_{0n}R_1) + R_2 J_0(k_{0n}R_2)] \int_d^{d+D} \frac{dz}{\left\{ 1 - \left[\left(d + \frac{D}{2} - z \right) \Big/ (D/2) \right]^2 \right\}^{1/3}} \right\}$$

Transforming Q_2 gives:

$$[A.6]\quad Q_2 = c_1\left\{(\epsilon_1^{-1}+\epsilon_0^{-1})\left[\left(\frac{R_2^2-R_1^2}{4}\right)\int_{-1}^{1}\left[\frac{J_0\left\{k_{0n}\left[\left(\frac{R_1+R_2}{2}\right)-\left(\frac{R_2-R_1}{2}\right)x\right]\right\}\,dx}{(1-x^2)^{1/3}}\right]\right.$$

$$-\frac{1}{4}(R_2-R_1)^2\int_{-1}^{1}\left[\frac{J_0\left\{k_{0n}\left[\left(\frac{R_1+R_2}{2}\right)-\left(\frac{R_2-R_1}{2}\right)x\right]\right\}x\,dx}{(1-x^2)^{1/3}}\right]$$

$$\left.+\epsilon_0^{-1}[2(R_2-R_1)D^2]^{1/3}\,[R_1J_0(k_{0n}R_1)+R_2J_0(k_{0n}R_2)]\int_0^{\pi/2}\cos^{1/3}x\,dx\right\}$$

Using the identity (12):

$$[A.7]\quad J_0(x+y)=J_0(x)J_0(y)+2\sum_{m=1}^{\infty}(-1)^mJ_m(x)J_m(y)$$

we can write:

$$[A.8]\quad J_0\left\{k_{0n}\left[\left(\frac{R_1+R_2}{2}\right)-\left(\frac{R_2-R_1}{2}\right)x\right]\right\}=J_0\left[k_{0n}\left(\frac{R_1+R_2}{2}\right)\right]J_0\left[k_{0n}\left(\frac{R_2-R_1}{2}\right)x\right]$$

$$+\sum_{m=1}^{\infty}J_m\left[k_{0n}\left(\frac{R_1+R_2}{2}\right)\right]J_m\left[k_{0n}\left(\frac{R_2-R_1}{2}\right)x\right]$$

where the identities:

$$[A.9]\quad J_0(-x)=J_0(x)$$

and:

$$[A.10]\quad J_m(-x)=(-1)^mJ_m(x)$$

were also used in deriving the expression [A.8]. It may be observed that:

$$\int_{-1}^{1}\frac{J_0(\lambda x)\,dx}{(1-x^2)^{1/3}}=0$$

due to the oddness of the integrand; therefore, the expression [A.6] becomes:

$$[A.11]\quad Q_2=c_1\left\{(\epsilon_1^{-1}+\epsilon_0^{-1})\left[\left(\frac{R_2^2-R_1^2}{2}\right)J_0\left[k_{0n}\left(\frac{R_1+R_2}{2}\right)\right]\int_0^{1}\frac{J_0\left[k_{0n}\left(\frac{R_2-R_1}{2}\right)x\right]dx}{(1-x^2)^{1/3}}\right.\right.$$

$$\left.+\left(\frac{R_2^2-R_1^2}{2}\right)\sum_{m=1}^{\infty}[1+(-1)^m]\,J_m\left[k_{0n}\left(\frac{R_1+R_2}{2}\right)\right]\int_0^{1}\frac{J_m\left[k_{0n}\left(\frac{R_2-R_1}{2}\right)x\right]dx}{(1-x^2)^{1/3}}\right]$$

$$\left.+\epsilon_0^{-1}\frac{[\Gamma(2/3)]^2}{2^{2/3}\Gamma(4/3)}[2(R_2-R_1)D^2]^{1/3}\,[R_1J_0(k_{0n}R_1)+R_2J_0(k_{0n}R_2)]\right\}$$

The integrals in [A.11] may not be expressed in closed form. Using the definition:

$$[A.12]\quad A_m(\lambda)\equiv\int_0^{1}\frac{J_m(\lambda x)\,dx}{(1-x^2)^{1/3}};\qquad m\geq 0$$

Then the integral Q_2 may be written compactly:

$$[A.13]\quad Q_2(k_{0n};R_1,R_2,D) = c_1\left\{\frac{1}{2}\left(\frac{1}{\epsilon_1}+\frac{1}{\epsilon_0}\right)(R_2^2-R_1^2)\left(J_0\left[k_{0n}\left(\frac{R_1+R_2}{2}\right)\right]A_0\left[k_{0n}\left(\frac{R_2-R_1}{2}\right)\right]\right.\right.$$
$$\left.+\,2\sum_{m=1}^{\infty} J_{2m}\left[k_{0n}\left(\frac{R_1+R_2}{2}\right)\right]A_{2m}\left[k_{0n}\left(\frac{R_2-R_1}{2}\right)\right]\right)+\frac{1}{\epsilon_0}\left(\frac{[\Gamma(2/3)]^2}{2^{1/3}\Gamma(4/3)}\right)$$
$$\left.\times\,[(R_2-R_1)D^2]^{1/3}[R_1J_0(k_{0n}R_1)+R_2J_0(k_{0n}R_2)]\right\}$$

Upon setting $k_{0n}=0$ and $\epsilon_1=\epsilon_0=1$ in [A.13], the expected limit:

$$Q_2(0;R_1,R_2,D) = Q_1(R_1,R_2,D)$$

is obtained.

(iii) $Q_3 = \int_0^\infty \rho\,d\rho \int_0^\infty dz\,J_0(k_{0n}\rho)\{\sigma_F(\rho)+\sigma_S(z)\}\sinh(k_{0n}z)$

The explicit form of Q_3 is:

$$[A.i4]\quad Q_3 = c_1\left\{(\sinh(k_{0n}d)+\sinh[k_{0n}(d+D)])\int_{R_1}^{R_2}\frac{\rho J_0(k_{0n}\rho)\,d\rho}{\left\{1-\left[\left(\frac{R_1+R_2}{2}-\rho\right)\Big/\left(\frac{R_2-R_1}{2}\right)\right]^2\right\}^{1/3}}\right.$$
$$\left.+\left(\frac{2(R_2-R_1)}{D}\right)^{1/3}[R_1J_0(k_{0n}R_1)+R_2J_0(k_{0n}R_2)]\int_d^{d+D}\frac{\sinh(k_{0n}z)\,dz}{\left\{1-\left[\left(d+\frac{D}{2}-z\right)\Big/(D/2)\right]^2\right\}^{1/3}}\right\}$$

The radial integral above has been worked out in the evaluation of Q_2. The second integral may be transformed as follows:

$$[A.15]\quad I(k_{0n};d,D) \equiv \int_d^{d+D}\frac{\sinh(k_{0n}z)\,dz}{\left\{1-\left[\left(d+\frac{D}{2}-z\right)\Big/(D/2)\right]^2\right\}^{1/3}}$$
$$= \frac{1}{4}D\exp\left[k_{0n}\left(d+\frac{D}{2}\right)\right]\int_0^\pi \exp\left(-\frac{1}{2}k_{0n}D\cos\theta\right)\sin^{1/3}\theta\,d\theta$$
$$-\frac{1}{4}D\exp\left[-k_{0n}\left(d+\frac{D}{2}\right)\right]\int_0^\pi \exp\left(\frac{1}{2}k_{0n}D\cos\theta\right)\sin^{1/3}\theta\,d\theta$$
$$= \frac{1}{4}D\left\{\exp\left[k_{0n}\left(d+\frac{D}{2}\right)\right]-\exp\left[-k_{0n}\left(d+\frac{D}{2}\right)\right]\right\}\sqrt{\pi}\left(\frac{4}{k_{0n}D}\right)^{1/6}\Gamma(2/3)\,I_{1/6}\left(\frac{k_{0n}D}{2}\right)$$

(ref. 13, entry 3.915.4)

$$= \frac{\sqrt{\pi}}{2}\Gamma(2/3)(4/k_{0n}D)^{1/6}D\sinh\left[k_{0n}\left(d+\frac{D}{2}\right)\right]I_{1/6}(k_{0n}D/2)$$

where $I_{1/6}$ is the modified Bessel function of the (1/6)th order.
Upon using the expressions [A.11] and [A.15], Q_3 may be written in the form:

$$[A.16]\quad Q_3(k_{0n};R_1,R_2,d,D) = c_1\left\{(\sinh(k_{0n}d)+\sinh[k_{0n}(d+D)])\left((R_2^2-R_1^2)\left(J_0\left[k_{0n}\left(\frac{R_1+R_2}{2}\right)\right]\right.\right.\right.$$
$$\left.\left.\left.\times\,A_0\left[k_{0n}\left(\frac{R_2-R_1}{2}\right)\right]+\sum_{m=1}^{\infty}J_{2m}\left[k_{0n}\left(\frac{R_1+R_2}{2}\right)\right]A_{2m}\left[k_{0n}\left(\frac{R_2-R_1}{2}\right)\right]\right)\right)$$

$$+ \frac{\sqrt{\pi}}{2}\Gamma(2/3)(4/k_{0n}D)^{1/6}[2(R_2 - R_1)D^2]^{1/3}[R_1J_0(k_{0n}R_1) + R_2J_0(k_{0n}R_2)]I_{1/6}(k_{0n}D/2)\sinh\left[k_{0n}\left(d + \frac{D}{2}\right)\right]\Bigg\}$$

Here A_0, A_m have been defined in [A.12].

Appendix II

Evaluation of the integrals Q_1, Q_2, Q_3 *for a disc with nonzero thickness*

(*i*) Using the expression [3.15], the definition of the Heaviside operator, and the properties of the Dirac delta function, Q_1 can be written as:

$$[B.1] \quad Q_1 = c_1\left\{2\int_0^R \frac{\rho\,d\rho}{[1 - (\rho/R)^2]^{1/3}} + \left(\frac{2R}{D}\right)^{1/3} R \int_d^{d+D} \frac{dz}{\left(1 - \left[\left(d + \frac{D}{2} - z\right)\Big/(D/2)\right]^2\right)^{1/3}}\right.$$

Using results from Appendix I it can be shown that:

$$[B.2] \quad Q_1(R,D) = c_1\left\{\frac{3R^2}{2} + \frac{[\Gamma(2/3)]^2}{2^{2/3}\Gamma(4/3)}(2RD^2)^{1/3}R\right\}$$

$$(ii) \quad Q_2 = c_1\left\{(\epsilon_1^{-1} + \epsilon_0^{-1})\int_0^R \frac{\rho J_0(k_{0n}\rho)\,d\rho}{[1 - (\rho/R)^2]^{1/3}} + \epsilon_0^{-1}\left(\frac{2R}{D}\right)^{1/3} RJ_0(k_{0n}R)\right.$$

$$\left.\times \int_d^{d+D} \frac{dz}{\left\{1 - \left[\left(d + \frac{D}{2} - z\right)\Big/(D/2)\right]^2\right\}^{1/3}}\right\}$$

Performing the required integrations gives:

$$[B.3] \quad Q_2(k_{0n};R,D) = c_1\left\{\Gamma(2/3)\left(\frac{1}{\epsilon_0} + \frac{1}{\epsilon_1}\right)\left(\frac{R^4}{2k_{0n}^2}\right)^{1/3} J_{2/3}(k_{0n}R) + \left(\frac{[\Gamma(2/3)]^2}{2^{2/3}\Gamma(4/3)}\right)\frac{(2RD^2)^{1/3}}{\epsilon_0} RJ_0(k_{0n}R)\right\}$$

(*iii*)

$$[B.4] \quad Q_3 = c_1\left\{(\sinh(k_{0n}d) + \sinh[k_{0n}(d + D)])\int_0^R \frac{\rho J_0(k_{0n}\rho)\,d\rho}{[1 - (\rho/R)^2]^{1/3}}\right.$$

$$\left.+ \left(\frac{2R}{D}\right)^{1/3} RJ_0(k_{0n}R)\int_d^{d+D} \frac{\sinh(k_{0n}z)\,dz}{\left\{1 - \left[\left(d + \frac{D}{2} - z\right)\Big/(D/2)\right]^2\right\}^{1/3}}\right\}$$

From results in Appendix I, the above expression becomes:

$$[B.5] \quad Q_3(k_{0n};R,d,D) = c_1\Gamma(2/3)\left\{2\left(\frac{R^4}{2k_{0n}^2}\right)^{1/3} J_{2/3}(k_{0n}R)(\sinh(k_{0n}d) + \sinh[k_{0n}(d + D)])\right.$$

$$\left.+ \frac{\sqrt{\pi}}{2}(2RD^2)^{1/3}R\left(\frac{4}{k_{0n}D}\right)^{1/6}\sinh\left[k_{0n}\left(d + \frac{D}{2}\right)\right]J_0(k_{0n}R)\,I_{1/6}(k_{0n}D/2)\right\}$$

Appendix III

Evaluation of the integrals Q_1, Q_2, Q_3 *for the infinitely thin disc*

Using the expression [3.17] and proceeding as in the Appendices I and II, Q_1 can be written:

$$[C.1] \quad Q_1 = c_1\int_0^R \frac{\rho\,d\rho}{[1 - (\rho/R)^2]^{1/2}} = c_1R^2$$

Also:

$$Q_2 = \frac{1}{2} c_1 (\epsilon_1^{-1} + \epsilon_0^{-1}) \int_0^R \frac{J_0(k_{0n}\rho)\rho \, d\rho}{[1 - (\rho/R)^2]^{1/2}}, \quad \text{or}$$

$$[C.2] \quad Q_2(k_{0n};R) = c_1 R^2 \left\{ \frac{1}{2} (\epsilon_1^{-1} + \epsilon_0^{-1}) \frac{\sin (k_{0n}R)}{k_{0n}R} \right\}$$

Similarly:

$$Q_3 = c_1 \sinh (k_{0n}d) \int_0^R \frac{J_0(k_{0n}\rho)\rho \, d\rho}{[1 - (\rho/R)^2]^{1/2}}, \quad \text{or:}$$

$$[C.3] \quad Q_3(k_{0n};R,d) = c_1 R^2 \left[\frac{\sin (k_{0n}R)}{k_{0n}R} \right] \sinh (k_{0n}d)$$